

Unlike Behavior of Natural Frequencies in Bending Beam Vibrations with Boundary Damping in Context of Bio-inspired Sensors

Carsten Behn
and Christoph Will

Department of Technical Mechanics
Ilmenau University of Technology, Germany
Email: carsten.behn@tu-ilmenau.de
Email: christoph.will@tu-ilmenau.de

Joachim Steigenberger

Institute of Mathematics
Ilmenau University of Technology, Germany
Email: joachim.steigenberger@tu-ilmenau.de

Abstract—In this paper, we introduce certain models which arise in investigating some vibration problems of bio-inspired, vibrissa-like sensor models. Some approaches to the modeling of the biological paragon vibrissa use rigid body models in which a rod-like vibrissa is supported by a combination of spring and damping elements modeling the viscoelastic properties of the follicle-sinus complex. However, all the rigid body models can only offer limited information about the functionality of the biological sensory system. Therefore, we deal with bending problems of continuous beam systems. We present various beams with different supports (clamped and pivoted with discrete viscoelastic couplings) which are to model the biological tissues. This is new in and different from literature. We focus on investigations of the natural frequency spectra of various systems. The knowledge of dynamical characteristics is important for the design of artificial sensors. A close examination of vibrissa-like beam models with boundary damping exhibits features which are unlike in comparison to classical vibration systems.

Keywords—Bending beam vibration; Boundary damping; Natural frequency; Bio-inspired sensor; Vibrissa.

I. INTRODUCTION

The classical Euler-Bernoulli beam is often used to analyze the vibration behavior of systems in technical disciplines like mechanical engineering, automotive engineering (e.g., power train vibration), microsystems technologies (e.g., cantilever vibration). In recent years, this classical model is used to model and to understand effects of vibrissa sensor systems in biomechanics [14]. This is the background of the work presented in the paper. Due to the biological paragon, we set up various mechanical models and analyze them in an analytical and numerical way. In contrast to works from literature [3] [17] [29], we focus on vibrissa dynamics, precisely, we try to get information about an obstacle contact in determining the spectrum of natural frequencies and calculate its shift according to an obstacle contact (sudden change of boundary conditions) [30]. In contrast to literature, we incorporate spring and damping elements, representing the biological tissue of animal skin and support of the vibrissa. This is rarely done in literature. Hence, we extend results in [21]. For this, we start an introduction to the biological paragon, describing its functionality, presenting the state of art in modeling animal vibrissae, and introduce the analytical treatment of transverse vibrations of beams due to [32] in the following.

A. Biological paragon animal vibrissa

Mice and rats use their vibrissae (in the mystacial pad) to acquire information about their surroundings. The vibrissa itself (made of dead material) is mainly used as a lever for the force transmission. But, in contrast to ordinary hairs, vibrissae are stiffer and have a (assumed hollow) conical shape [4]. The mystacial vibrissae are arranged in an array of columns and rows around the snout, see Fig. 1 and [31]. Each

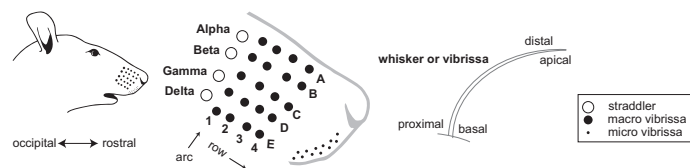


Figure 1. Schematic drawing of the mystacial pad, [31], arranged by D. Voges (TU Ilmenau).

vibrissa is embedded in and supported by its own follicle-sinus complex (FSC). The FSC is characterized by its exceptional arrangement of blood vessels, neural connections and muscles. It is presumed that the rodents can control the viscoelastic properties of the vibrissa's support by regulating the blood supply to the sinus (like a blood sac) [5]. The functionality of these vibrissae vary from animal to animal and is best developed in rodents, especially in mice and rats [16]. The detection of contact forces is made possible by the pressure-sensitive mechanoreceptors in the support of the vibrissa (i.e., FSC), see Fig. 2. These mechanoreceptors are stimulated due to the vibrissa displacements in the FSC. The nerves transmit the information through several processing units to the Central Nervous System (CNS). The receptor cells offer the fundamental principle 'adaptation'. The muscle-system, see Fig. 3 (adapted from [5] [6] [33] [12]) enables the rodents to use their vibrissae in two different ways (modes of operation): In the *passive mode*, the vibrissae are being deflected by external forces (e.g., wind). They return to their rest position passively — thus without any muscle activation, just via the fibrous band. In the *active mode*, the vibrissae are swung back- and forward by alternate contractions of the intrinsic and extrinsic muscles (with different frequencies and amplitudes). By adjusting the frequency and amplitude of the oscillations, the rodents are able to investigate object surfaces and shapes amazingly fast and with high precision [13]. *But*, how the

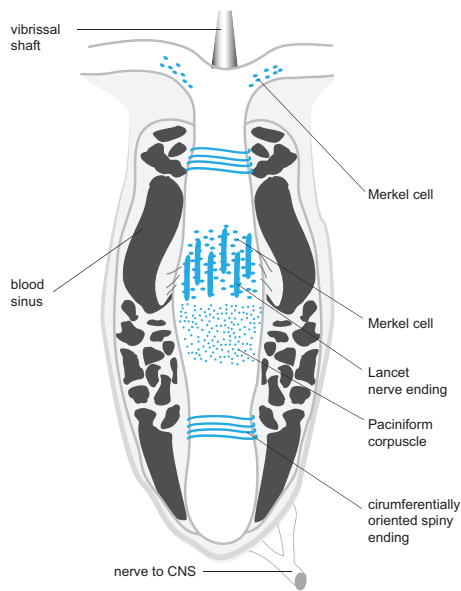


Figure 2. FSC of a vibrissa with various types of receptors (blue) [2]. Adapted from [7] [23], arranged by D. Voges (TU Ilmenau).

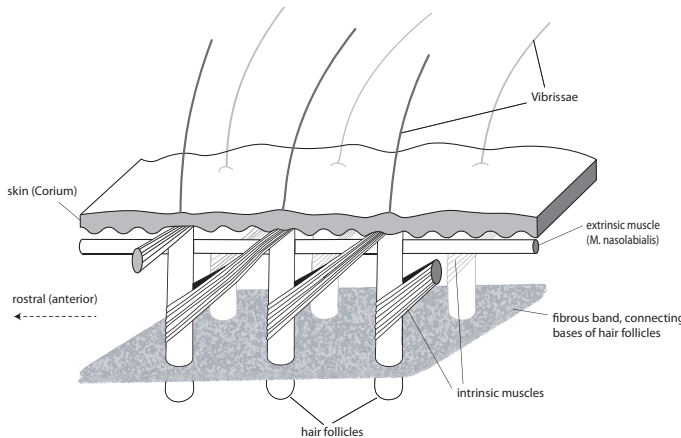


Figure 3. Schematic drawing of neighboring mystacial follicles [2]. Arranged by D. Voges (TU Ilmenau).

animals convert these multiple contacts with single objects into coherent information about their surroundings is still unclear. And it is not of main interest from our point of view: the tenor of our investigations is from bionics. The main focus is not on “copying” the solution from biology/animality, rather on detecting the main features, functionality and algorithms of the considered biological systems to implement them in (here: mechanical) models and to develop ideas for prototypes. Therefore, this biological sensor system is highly interesting for applications in the field of autonomous robotics, since tactile sensors can offer reliable information, where conventional sensors fail (in dark, smoky or noisy environments).

B. State of art in modeling vibrissa-like sensors

Since the author in [24] tried to determine the position of a robot arm with vibrissa-like sensors (made of guitar strings), the demand for technical vibrissae grew steadily. In the meantime, these tactile sensors often complement or even

replace optical sensors (as mentioned above) in their two main fields of application: flow measurements in micro technology and autonomous robotics. Especially in the latter field, technical vibrissae are currently just used to avoid collisions (merely used as contact sensors with a binary output [22]). In the last decade, the number of scientific works in which the capabilities of the tactile sensors were improved, grew significantly. As in 1996 the development of robots equipped with artificial vibrissae and driving along walls [15], was seen as a considerable achievement, the recently developed robots with a similar configuration managed to distinguish objects on the basis of their surface texture [8] [27] [34] [9] [19], or to determine form and position of nearby objects [26]. In the majority of papers found in literature, the development of innovative technical whiskers was poorly based on mechanical models of the vibrissa. In order to analyze the mechanical and especially the dynamical behavior of the vibrissa, the physical principles of the paradigm have to be identified. Therefore, abstract technical models, which describe the biological example in detail and are suitable to be analyzed using engineering and scientific methods, are sought. Usually two types of models are used to analyze the mechanical behavior of the vibrissa:

- *Rigid body models* form the vibrissa as a stiff, inelastic body. Such models have the advantage of a simple mathematical description and solution. Furthermore, these models can easily be used to analyze the influence of varying viscoelastic supports. However, neglecting the inherent elasticity of the vibrissa implies a questionable oversimplification of the biological example.
- *Continuum models* are closer to the biological paradigm, as the tactile hair is implemented as an elastic beam. They are thus able to take the inherent dynamical behavior and the bending stiffness of the biological vibrissa into account.

An intensive literature overview of technical vibrissa models (rigid body and continuum) has been given in [2]. In the following we summarize the relevant models thereof without any valuation:

Birdwell et al. [3] - Model analyzing the bending behavior of natural vibrissae

- ⊕ suitable to analyze the bending behavior
- ⊖ Linearized model: only valid for small deflections
- ⊕ Consideration of the conical shape of the vibrissa
- ⊖ Neglecting the support’s compliance
- ⊕ Finding: Shape of the beam influences the bending behavior
↔ not negligible
- ⊕ Finding: Young’s modulus of natural vibrissae varies

Birdwell et al. [3] - Model to determine clamping torques

- ⊖ Linearized model only valid for small deflections
- ⊕ Consideration of the conical vibrissa shape
- ⊖ Neglecting the support’s compliance
- ⊕ Finding: influence of the natural pre-curvature of the vibrissa is negligible

Scholz and Rahn [25] - Model for profile sensing with an actuated vibrissa

- ⊕ Implementation of the active mode
- ⊖ Neglecting the support's compliance

Neimark et al. [18], Andermann et al. [1] - Model for the determination of the support's influence on the resonance properties of natural vibrissae

- ⊕ Experimental measurements of vibrissae's resonance frequencies
- ⊖ dubious results during numerical evaluations
 - ↔ due to constant Young's modulus taken for all vibrissae
- ⊕ Finding: massive influence of the support on the resonance frequencies
- ⊖ Determination only of the first frequencies of the vibrissae
- ⊕ Finding: geometrically distributed sensitivity in the vibrissa array
- ⊕ Finding: transduction and processing of the frequency provoking stimuli to the CNS
 - ↔ Resonance frequencies contain relevant information

There are a lot of more works concerning bending problems of vibrissa-like beams, but in context of quasi-statically object scanning and not in context of dynamical treatment, e.g., in [20].

C. Criticism and Goal of Investigations

Most of the models in literature, in particular the rigid body models, are just results of anatomic investigations. They do not directly aim at bionic applications. Further on, some models are very exact, but too complex to gain deeper insight the system to identify the essential mechanical elements. On the other hand, in particular, concerning continuum beam models, the level of mathematical investigations is rather low:

- linear bending theory with very simple (obvious) conclusions,
- mixing of linear and nonlinear theories, and
- using boundary-value problems (BVP) which do not match the real objects sufficiently.

Based on the mentioned criticisms the **global goal** is to *present models more transparent and to use more stringent mechanics and mathematical analysis to exploit them*. The goal is **not** to recreate an exact copy of the biological system, but to *implement in a mechanical model the specific characteristics of the vibrissa needed for the detection of useful information in challenging surroundings (principle goal of theoretical bionics)*.

A lot of works offer models consisting of beams or rigid rods for the vibrissa and mapping the arrangement of the muscles needed for the different modes of operation by viscoelastic supports. Some of those models consider a complete row of vibrissae. These models are too complex to handle and are not investigated further in those papers. Our aim is to set up simple models for the investigations first, and then to increase the complexity by adding more viscoelastic supports and to increase the degree of freedom. The viscoelastic support is very important since we have to model the compliance of the FSC and the skin, which was omitted in [18]. The boundary conditions there did not match reality, and the authors considered only the first natural frequency. We will focus on the

determination of a part of the natural frequency spectrum of the vibrissa models to obtain a characteristic change depending on the change of the viscoelastic support. For these investigations we derive the equations of motion analytically to treat them with numerical tools: we try to detect useful information from the surroundings, where we focus on *changes* of environmental signals. This is quite easier to organize since the animals, more precisely, the CNS has problems in determination absolute values [3].

We point out, that we focus on a single vibrissa and not on a tuft of various vibrissae.

II. CONTINUUM BEAM MODELS

We will present various approaches to implement and to determine the basic features of animal vibrissae as mentioned in Subsection I-A.

Here, we will focus on the mechanical properties and the dynamic behavior of the vibrissa beam models. The processing of the stimulus and the corresponding analysis of different control strategies are **not** discussed here. Furthermore, the investigations are addressed to a single vibrissa – the interaction between the different vibrissae in the mystacial pad is **not** taken into account.

The classical differential equation for small bending vibrations of beams (linear Euler-Bernoulli theory) is the basis of the investigations. We will set up and analyze various vibrissa beam models with different supports using discrete and continuously distributed spring and damping elements to mimic tissues of FSC and skin. Following [18], we focus on the determination of the natural frequency spectrum of such beams analytically and numerically, while varying the viscoelastic properties of the support. We will not focus on static bending problems in the following.

Starting point and motivation of the following investigations are multiple **hypotheses** concerning the **functionality of the vibrissa**:

- The elasticity and the conical shape of the hair are relevant for the functionality of the vibrissa [3].
- The viscoelastic properties of the support (see the FSC) are controlled by the blood pressure in the blood sinus [5] [4].
- The vibrissae are excited with or close to their resonance frequencies during the active mode [18] [1].

Following these hypotheses, the primary tasks now are:

- to investigate the influence of elasticity and conical shape on the vibration characteristics of the vibrissa by analyzing its natural frequency spectrum;
- to analytically examine innovative models of a flexible vibrissa with a viscoelastic support which fit the real object and its support better than models in literature.

A. Introduction to Transversal Bending Beam Vibrations

Let us start with the following example: a one-sided clamped beam with elastic support (spring stiffness c) at the

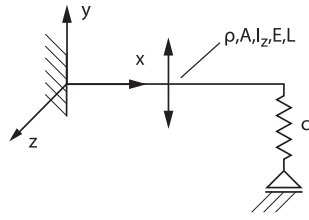


Figure 4. One-sided clamped beam with elastic end support.

end, see Fig. 4. The beam has length L , Young's modulus E , density ρ , constant cross section area A and second moment of area I_z . We are seeking for the first five natural frequencies.

Remark II.1. We focus on the first five natural frequencies of the spectrum because of

1. *mathematical reasons: the first five natural frequencies will form a good approximation basis of the Fourier series of the solution made by the method of separation of variables; and*
2. *physical meanings – higher natural frequencies are too large, whereas only lower ones are perceptible by means of tactile sense.*

The well-known equation of motion for free vibrations of a beam with small deformations, as in Fig. 4, is:

$$\ddot{v}(x, t) + k^4 v''''(x, t) = 0, \quad \text{with } k^4 := \frac{E I_z}{\rho A}, \quad (1)$$

where the function $v(x, t)$ describes the vertical displacement at point x and at time t .

The partial differential equation (PDE) (1) and the following boundary conditions

- ①: $v(0, t) = 0 \quad \forall t \geq 0$
 - ②: $v'(0, t) = 0 \quad \forall t \geq 0$
 - ③: $v''(L, t) = 0 \quad \forall t \geq 0$
 - ④: $v'''(L, t) E I_z - c v(L, t) = 0 \quad \forall t \geq 0$
- form a BVP.

Now, we apply the *method of separation of variables*, i.e., we are seeking for special solutions of structure

$$v(x, t) = X(x) \cdot T(t) \quad \forall (x, t). \quad (2)$$

Substitution into (1) yields two ordinary differential equations (ODEs)

$$\frac{\ddot{T}(t)}{T(t)} = -\mu^2, \quad (3)$$

$$-k^4 \frac{X''''(x)}{X(x)} = -\mu^2. \quad (4)$$

The general solution of 3 is

$$T(t) = \underline{B}_1 e^{i\mu t} + \underline{B}_2 e^{-i\mu t}, \quad \underline{B}_1, \underline{B}_2 \in \mathbb{C}. \quad (5)$$

The solution of 4 is:

$$X(x) = C_1 \cos(\lambda x) + C_2 \sin(\lambda x) + C_3 \cosh(\lambda x) + C_4 \sinh(\lambda x). \quad (6)$$

with $C_1, C_2, C_3, C_4 \in \mathbb{C}$ and

$$\lambda^4 := \frac{\mu^2}{k^4}, \quad k^4 := \frac{E I_z}{\rho A}. \quad (7)$$

This shape solution (6) together with the formulated four boundary conditions form an eigenvalue problem (EVP) in the following. We get $\forall t \geq 0$

- ① $T(t) (C_1 + C_3) = 0$
- ② $T(t) \lambda (C_2 + C_4) = 0$
- ③ $T(t) \lambda^2 (-C_1 \cos(\lambda L) - C_2 \sin(\lambda L) + C_3 \cosh(\lambda L) + C_4 \sinh(\lambda L)) = 0$
- ④ $E I_z T(t) \lambda^3 (C_1 \sin(\lambda L) - C_2 \cos(\lambda L) + C_3 \sinh(\lambda L) + C_4 \cosh(\lambda L)) - c T(t) (C_1 \cos(\lambda L) + C_2 \sin(\lambda L) + C_3 \cosh(\lambda L) + C_4 \sinh(\lambda L)) = 0$

$T(t)$ drops, and a system of homogenous linear equations results with a coefficient matrix (8).

Since we are seeking for non-trivial solutions, we claim the singularity of the coefficient matrix: $\det(M) = 0$. Introducing a ratio of elasticity

$$\gamma_c := \frac{c}{c_S} = \frac{c}{\frac{E I_z}{L^3}} = \frac{c L^3}{E I_z}$$

we obtain the characteristic eigenvalue equation

$$\lambda^3 L^3 (1 + \cosh(\lambda L) \cos(\lambda L)) + \gamma_c (\cosh(\lambda L) \sin(\lambda L) - \cos(\lambda L) \sinh(\lambda L)) = 0 \quad (9)$$

Remark II.2. Before solving (9) we check it in setting

- $c = 0$: we get $1 + \cosh(\lambda L) \cos(\lambda L) = 0$, which forms the eigenvalue equation of an one-sided clamped / free end beam;
- $c \rightarrow +\infty$: we get $\cosh(\lambda L) \sin(\lambda L) - \cos(\lambda L) \sinh(\lambda L) = 0$, which arises for a clamped beam with bearing.

Now, we present some numerical calculations. We are varying $\gamma_c = 0, 0.1, 1, +\infty$ and derive the natural frequencies of a steel beam and of a B2 vibrissa, see Fig. 1, using the following parameters:

- steel beam: $E = 210 \text{ GPa}$, $\rho = 7850 \frac{\text{kg}}{\text{m}^3}$;
- B2 vibrissa: $E = 2.3 \text{ GPa}$, $\rho = 238.732 \frac{\text{kg}}{\text{m}^3}$;
- geometric parameters: $d = 0.2 \text{ mm}$, $I_z = \frac{\pi}{64} d^4$, $A = \frac{\pi}{4} d^2$, $L = 40 \text{ mm}$.

The following tables present the first five eigenvalues λ_j , natural frequencies ω_j in rad/s and frequencies f_j in Hz for a steel beam and a B2 vibrissa.

$$M(\lambda) := \begin{pmatrix} 1 & \vdots & 0 & \vdots & 1 & \vdots & 0 \\ \dots & \dots & \dots & \dots & \dots & \dots & \dots \\ 0 & \vdots & \lambda & \vdots & 0 & \vdots & \lambda \\ \dots & \dots & \dots & \dots & \dots & \dots & \dots \\ \cos(\lambda L) \lambda^2 & \vdots & \sin(\lambda L) \lambda^2 & \vdots & \cosh(\lambda L) \lambda^2 & \vdots & \sinh(\lambda L) \lambda^2 \\ \dots & \dots & \dots & \dots & \dots & \dots & \dots \\ EI_z \sin(\lambda L) \lambda^3 & \vdots & -EI_z \cos(\lambda L) \lambda^3 & \vdots & EI_z \sinh(\lambda L) \lambda^3 & \vdots & EI_z \cosh(\lambda L) \lambda^3 \\ -c \cos(\lambda L) & \vdots & -c \sin(\lambda L) & \vdots & -c \cosh(\lambda L) & \vdots & -c \sinh(\lambda L) \end{pmatrix} \quad (8)$$

TABLE I. CALCULATION FOR $\gamma_c = 0$.

j	λ_j	steel beam		B2 vibrissa	
		ω_j	f_j	ω_j	f_j
1	1.875 $\frac{1}{L}$	568.297	90.447	733.807	54.279
2	4.694 $\frac{1}{L}$	3561.458	566.824	4598.693	340.159
3	7.855 $\frac{1}{L}$	9972.187	1587.123	12876.473	952.454
4	10.996 $\frac{1}{L}$	19541.506	3110.127	25232.748	1866.429
5	14.137 $\frac{1}{L}$	32303.509	5141.263	41711.541	3085.341

TABLE II. CALCULATION FOR $\gamma_c = 1$.

j	λ_j	steel beam		B2 vibrissa	
		ω_j	f_j	ω_j	f_j
1	2.010 $\frac{1}{L}$	653.008	103.929	843.189	62.369
2	4.704 $\frac{1}{L}$	3576.197	569.169	4617.724	341.566
3	7.857 $\frac{1}{L}$	9977.433	1587.958	12883.248	952.955
4	10.996 $\frac{1}{L}$	19544.181	3110.553	25236.203	1866.685
5	14.138 $\frac{1}{L}$	32305.127	5141.521	41713.630	3085.496

TABLE III. CALCULATION FOR $\gamma_c = +\infty$.

j	λ_j	steel beam		B2 vibrissa	
		ω_j	f_j	ω_j	f_j
1	3.927 $\frac{1}{L}$	2492.061	396.624	3217.846	238.019
2	7.069 $\frac{1}{L}$	8075.874	1285.315	10427.881	771.335
3	10.210 $\frac{1}{L}$	16849.666	2681.708	21756.941	1609.329
4	13.352 $\frac{1}{L}$	28813.927	4585.879	37205.657	2752.048
5	16.493 $\frac{1}{L}$	43968.656	6997.829	56774.030	4199.492

Increasing γ_c leads to increasing ω_j , see Table I to III. Let us further point out, that these first investigations of a simple beam model are rather obvious. In the following we will increase the level of complexity.

B. Bending Beam Vibrations with vibrissa-like Support

Here, we focus on various supports (no clamps) of the vibrissa beam model. In order to do the following investigations analytically, we neglect the conical shape of the vibrissa with respect to the complex structure of the arising PDE. We focus on cylindrical beams.

First vibrissa beam models are presented in Figs. 5 and 6. These models present a cylindrical pivoted beam with various elastic couplings. The analytical investigations are carried out in formulating the boundary value problems (BVPs) for each section of the beam. The arising eigenvalue problems could be treated analytically in parts.

But, all models offer the same drawback: the ‘pivot’ is the base of the vibrissa, this does not match the reality. Therefore, we modify these models: first we shifted the pivot, and second we added some viscous properties to the support. This results in the following models, shown in Figs. 7 and 8. The BVPs of the oscillating problems are formulated in the following:

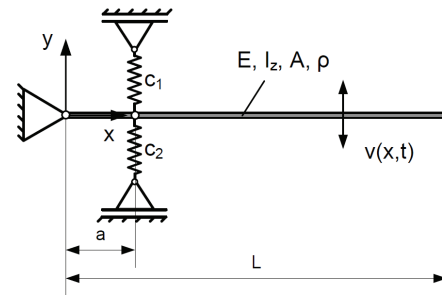


Figure 5. Pivoted vibrissa beam model with modeled skin support (one level of elasticity), [2].

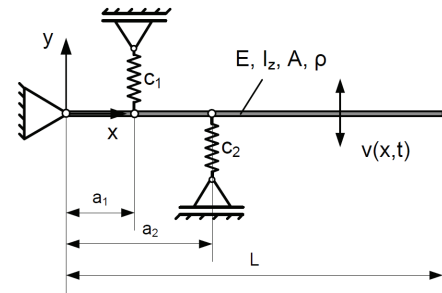


Figure 6. Pivoted vibrissa beam model with two levels of elasticity (FSC and skin), [2].

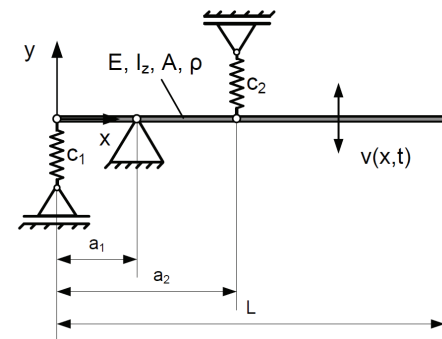


Figure 7. Undamped vibrissa beam model with modeled skin and FSC support, [2].

- undamped model in Fig. 7:
PDEs: $\ddot{v}_i(x,t) + k^4 v_i''''(x,t) = 0$, with $k^4 := \frac{E I_z}{\rho A}$, $i = 1, 2, 3$,

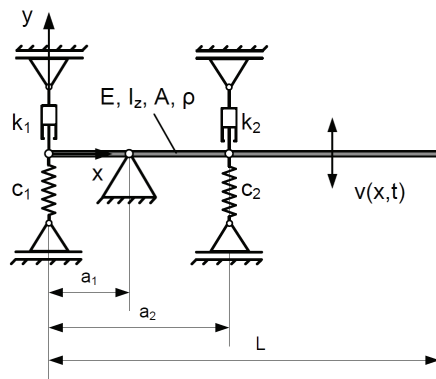


Figure 8. Damped vibrissa beam model with modeled skin and FSC support, [2].

boundary conditions:

$$\begin{aligned}
 v_1''(0, t) &= 0, \\
 -E I_z v_1'''(0, t) - c_1 v_1(0, t) &= 0, \\
 v_1(a_1, t) &= v_2(a_1, t), \\
 v_1(a_1, t) &= 0, \\
 v_1'(a_1, t) &= v_2'(a_1, t), \\
 v_1''(a_1, t) &= v_2''(a_1, t), \\
 v_2(a_2, t) &= v_3(a_2, t), \\
 v_2'(a_2, t) &= v_3'(a_2, t), \\
 v_2''(a_2, t) &= v_3''(a_2, t), \\
 E I_z (v_2'''(a_2, t) - v_3'''(a_2, t)) - c_2 v_2(a_2, t) &= 0, \\
 v_3(L, t) &= 0, \\
 v_3'''(L, t) &= 0
 \end{aligned}$$

- damped model in Fig. 8:
PDEs: $\ddot{v}_i(x, t) + k^4 v_i''''(x, t) = 0$, with $k^4 := \frac{E I_z}{\rho A}$, $i = 1, 2, 3$,
boundary conditions:

$$\begin{aligned}
 v_1''(0, t) &= 0, \\
 -E I_z v_1'''(0, t) - c_1 v_1(0, t) - k_1 v_1(0, t) &= 0, \\
 v_1(a_1, t) &= v_2(a_1, t), \\
 v_1(a_1, t) &= 0, \\
 v_1'(a_1, t) &= v_2'(a_1, t), \\
 v_1''(a_1, t) &= v_2''(a_1, t), \\
 v_2(a_2, t) &= v_3(a_2, t), \\
 v_2'(a_2, t) &= v_3'(a_2, t), \\
 v_2''(a_2, t) &= v_3''(a_2, t), \\
 E I_z (v_2'''(a_2, t) - v_3'''(a_2, t)) - c_2 v_2(a_2, t) - k_2 v_2(a_2, t) &= 0, \\
 v_3(L, t) &= 0, \\
 v_3'''(L, t) &= 0,
 \end{aligned}$$

To investigate the dependence of the natural frequencies on the system parameters, the eigenvalue problems (EVPs) are derived analytically (linear equations with zero determinant) and solved numerically for various cases. The following two examples illustrate some results.

Example II.3. Let us remind the comparison of a steel beam and a B2 vibrissa. Due to some techniques we are able to handle discrete damping terms to analytically derive the EVP, which then can be solved numerically. There are no problems in case of small damping coefficients, due to the biological

paradigm.

We set

- the geometric parameters $a_1 = 3$ mm, $a_2 = 4$ mm, $r = 0.1$ mm, and $L = 40$ mm;
- the support parameters for the FSC $c_1 = c_{\text{FSC}} = 80 \frac{\text{N}}{\text{m}}$ and $k_1 = d_{\text{FSC}} = 0.5 \frac{\text{Ns}}{\text{m}}$;
- and for the skin $c_2 = c_{\text{skin}} = 5.7 \frac{\text{N}}{\text{m}}$ and $k_2 = d_{\text{skin}} = 0.2 \frac{\text{Ns}}{\text{m}}$.

We get the results in Tables IV and V, where we present the first five eigenvalues λ_j , the first five natural frequencies ω_j in rad/s, and the decay rate δ_j in 1/s for both undamped and damped

- steel beam: parameters $E = 210$ GPa and $\rho = 7850 \frac{\text{kg}}{\text{m}^3}$, and
- B2 vibrissa: parameters: $E = 2.3$ GPa and $\rho = 238.732 \frac{\text{kg}}{\text{m}^3}$.

TABLE IV. CALCULATION FOR THE STEEL BEAM.

j	undamped		damped		
	λ_j	ω_j	λ_j	ω_j	δ_j
1	3.946	2517.314	$2.017 - 0.271 I$	645.851	176.755
2	7.448	8965.159	$4.941 - 0.085 I$	3944.771	135.721
3	10.800	18852.940	$8.297 - 0.005 I$	11126.480	129.665
4	14.004	31698.644	$11.650 + 0.068 I$	21936.355	257.106
5	16.934	46348.499	$15.023 + 0.150 I$	36477.396	727.763

TABLE V. CALCULATION FOR THE B2 VIBRISSA.

j	undamped		damped		
	λ_j	ω_j	λ_j	ω_j	δ_j
1	1.990	384.836	$1.993 + 0.033 I$	385.694	12.594
2	4.988	2416.865	$5.151 + 0.067 I$	2577.281	66.675
3	8.354	6779.153	$8.651 + 0.047 I$	7270.715	78.835
4	11.703	13306.010	$12.119 + 0.037 I$	14267.203	87.093
5	15.058	22027.360	$15.586 + 0.031 I$	23599.899	95.129

Considering the steel beam, the (natural) frequencies shrink if we focus on a damped system, as expected. But, we observe (see Table V) an unlike behavior simulating the B2 vibrissa as the (natural) frequencies increase in the damped system. This contradicts the classical assertions. The reason for this is a little bit unclear, we shall have a closer look to the modes of the beams.

Further, we hint to some problems in using discrete damping elements in the next Subsection II-C.

Short summary:

- ⊖ Neglecting the conical shape of the vibrissa
- ⊕ Consideration of the support's compliance
 - at skin level
 - at the level of the FSC
- ⊕ Finding: massive influence of the support on the natural frequencies
- ⊕ Finding: influence of damping elements in the support
 - ↔ massive for the 1st natural frequency
 - ↔ but: unlike behavior of the natural frequencies

C. Beam with discrete damping elements

To clarify the unlike effects of the foregoing subsection, we deal with a 'simple' problem to investigate the influence

of discrete damping elements. We consider a cylindrical, one-sided clamped beam which is viscoelastically supported at the end, see Fig. 9. The well-known PDE from the linear

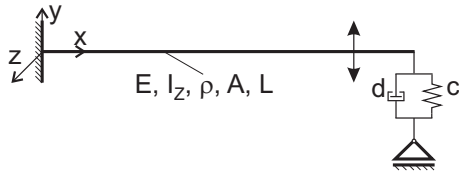


Figure 9. Clamped beam with viscoelastic end support.

Euler-Bernoulli theory is (1), which forms with the boundary conditions

$$\begin{aligned} v(0, t) &\equiv 0 \\ v'(0, t) &\equiv 0 \\ v''(L, t) &\equiv 0 \\ E I_z v'''(L, t) - d \dot{v}(L, t) - c v(L, t) &\equiv 0, \end{aligned}$$

a BVP.

The handling of the last boundary condition results in

$$E I_z X'''(L) - c X(L) = \pm i d \lambda^2 k^2 X(L).$$

All conditions lead to the coefficient matrix (10) of the homogenous systems whose singularity yields the eigenvalue equation:

$$\begin{aligned} \det(A(\lambda)) &= -E I_z \lambda^3 \\ &- E I_z \cos(\lambda L) \cosh(\lambda L) \lambda^3 \\ &\pm i d k^2 \sin(\lambda L) \cosh(\lambda L) \lambda^2 \\ &- c \sin(\lambda L) \cosh(\lambda L) \\ &\mp i d k^2 \cos(\lambda L) \sinh(\lambda L) \lambda^2 \\ &+ c \cos(\lambda L) \sinh(\lambda L) = 0. \quad (11) \end{aligned}$$

Remark II.4. At this stage, we could check this equation in concluding well-known eigenvalue equations: setting $\{d = 0, c = 0\}$, or $\{d = 0, c > 0\}$, or $\{d = 0, c \rightarrow +\infty\}$ results in the equations presented in [10] or [32].

Introducing the dimensionless parameters

$$\begin{aligned} \alpha_c &:= \frac{c}{E I_z} \\ \alpha_d &:= \frac{L d}{\sqrt{\rho A E I_z}}, \end{aligned}$$

we determine the first three natural frequencies in varying α_c and α_d . We get the following Figs. 10 to 12.

For fixed α_c and varying α_d , there are parameter ranges of α_c where we get an expected and unexpected behavior of the first natural frequency, see Fig. 10:

- $\alpha_c \in [0, 17]$: the natural frequency breaks down to zero for increasing α_d ;
- $\alpha_c \in [18, 23]$: first, the natural frequency increases and then breaks down to zero;
- $\alpha_c > 23$: the natural frequency just increases.

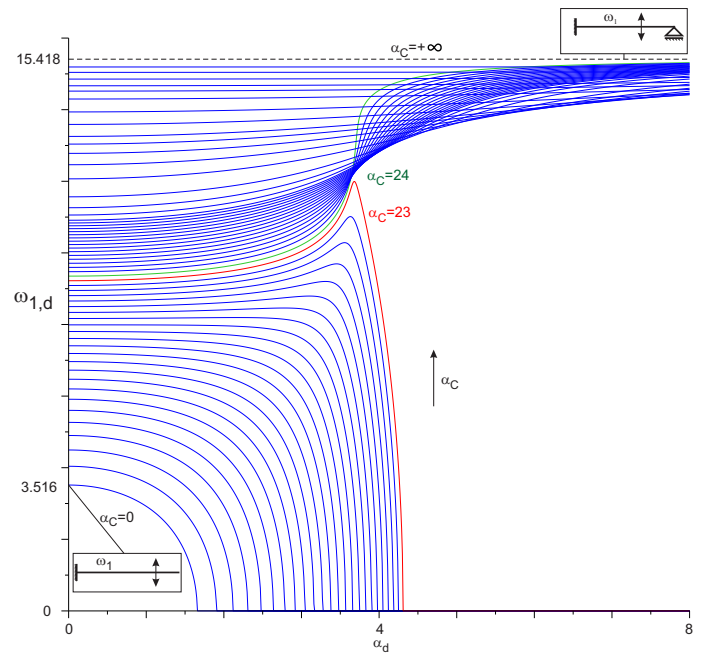


Figure 10. First natural frequency of the beam model $\omega_{1,d}$ in $\sqrt{\frac{E I_z}{\rho A L^4}}$ in dependence on α_c and α_d .

On the other hand, for fixed α_d and varying α_c , we observe the following:

- $\alpha_d \in [0, 3.5]$: increasing α_c leads to an increase of the natural frequency;
- $\alpha_d > 3.5$: an increase of α_c results first in a decrease and then in an increase of the natural frequency.

This may explain the behaviors of the natural frequencies in Example II.3.

Similar effects can be observed in Figs. 11 and 12.

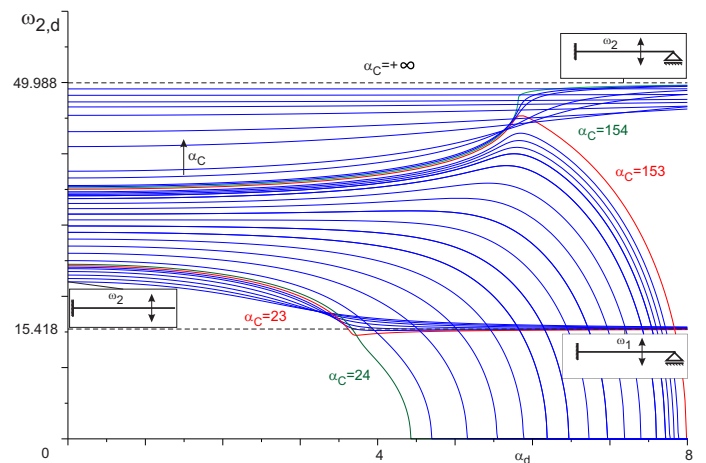


Figure 11. Second natural frequency of the beam model $\omega_{2,d}$ in $\sqrt{\frac{E I_z}{\rho A L^4}}$ in dependence on α_c and α_d .

It seems that some bifurcation is happening there. This has to be checked in future.

Former investigations on similar beam models are done in

$$A(\lambda) := \begin{pmatrix} 1 & \vdots & 0 & \vdots & 1 & \vdots & 0 \\ \dots & \dots & \dots & \dots & \dots & \dots & \dots \\ 0 & \vdots & \lambda & \vdots & 0 & \vdots & \lambda \\ \dots & \dots & \dots & \dots & \dots & \dots & \dots \\ EI_z \sin(\lambda L) \lambda^2 & \vdots & -EI_z \cos(\lambda L) \lambda^2 & \vdots & EI_z \sinh(\lambda L) \lambda^2 & \vdots & EI_z \cosh(\lambda L) \lambda^2 \\ \pm i d \lambda^2 k^2 \cos(\lambda L) & \vdots & \pm i d \lambda^2 k^2 \sin(\lambda L) & \vdots & \pm i d \lambda^2 k^2 \cosh(\lambda L) & \vdots & \pm i d \lambda^2 k^2 \sinh(\lambda L) \\ -c \cos(\lambda L) & \vdots & -c \sin(\lambda L) & \vdots & -c \cosh(\lambda L) & \vdots & -c \sinh(\lambda L) \\ \dots & \dots & \dots & \dots & \dots & \dots & \dots \\ -\cos(\lambda L) \lambda^2 & \vdots & -\sin(\lambda L) \lambda^2 & \vdots & \cosh(\lambda L) \lambda^2 & \vdots & \sinh(\lambda L) \lambda^2 \end{pmatrix} \quad (10)$$

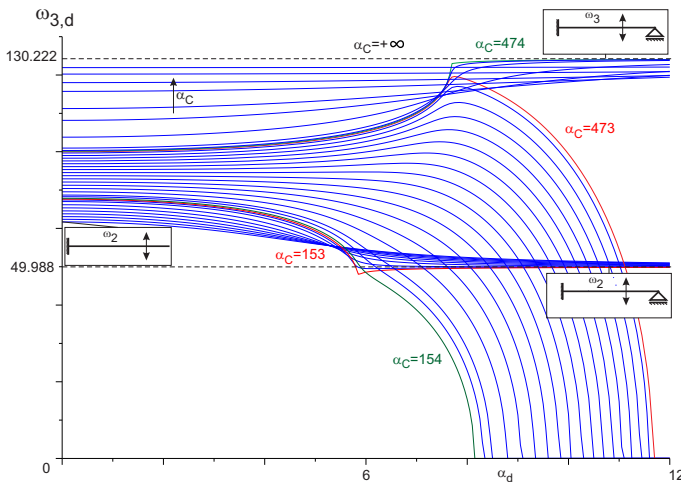


Figure 12. Third natural frequency of the beam model $\omega_{3,d}$ in $\sqrt{\frac{E I_z}{\rho A L^4}}$ in dependence on α_c and α_d .

[11], with focus on eigenvalues, and with focus on vibration amplitudes. But, no one derived the above curves of the behavior of natural frequencies.

III. CONCLUSION

The goal of this contribution was to present the theoretical context needed to examine the mechanical and in particular the dynamical characteristics of the biological vibrissa. Moreover, these theoretical aspects were to be interpreted with respect to the biological vibrissa, as well as for a technical implementation of it. Inspired by this biological sensory system, several types of mechanical models were developed based on findings in the literature.

The second focus was on the modeling of the vibrissa as a *continuous system*: bending vibrations of beams. There, the main focus of the studies lay on the examination of the influence of the tactile hair compliance and the viscoelastic support on the oscillation characteristics of the vibrissa. The conical form was neglected until now.

The influence of the viscoelastic support of the vibrissa has been examined using various abstract models in which the vibrissa was modeled as a thin, cylindrical, flexible beam. The viscoelastic properties of the FSC and the skin were implemented by using spring and damping elements.

The damping element significantly increased the complexity of the differential equations and led to a surprising phenomenon: there exist some natural frequencies which break down to zero for a certain range of parameters. This fact is well-known in 1-DoF systems (i.e., strong damping, creeping behavior). The study demonstrated that the oscillation behavior of an elastic beam differs remarkably from the behavior of such a classical system:

- The natural frequencies may increase with growing boundary damping.
- For specific damping parameter values, the natural frequencies grow for decreasing boundary stiffness.

Some similar effects on and the behavior of the natural frequencies can be observed in analyzing the model presented in Fig. 13. For a fixed parameter set of the system, except the

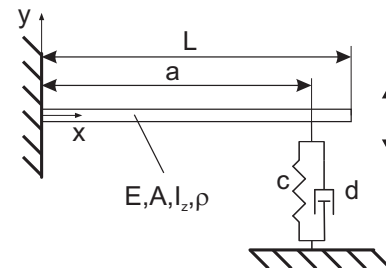


Figure 13. One-sided clamped beam with viscoelastic support.

distance a of the viscoelastic support to the clamping, we get the following results of the first three natural frequency of the beam, see Fig. 14 to 16, which offer already the same unlike behavior as the example above.

But, theories gained from the simplified linear Euler-Bernoulli theory are only valid for small deflections and deformations. If one considers a vibrissa beam in passive mode, then it may be questionable if this theory is really qualified for the investigations, see large bending deformations. Inspecting these vibrissa configurations, one could clearly observe that the vibrissa in passive mode suffers large deformations. Hence, the linear Euler-Bernoulli theory is not qualified to determine the natural frequencies since it describes the bending behavior for small deformations. We have to turn to a nonlinear theory: Timoshenko theory or nonlinear Euler-Bernoulli theory. We will arrive at more realistic models and description of these models, which then are closer to the biological paradigm. An

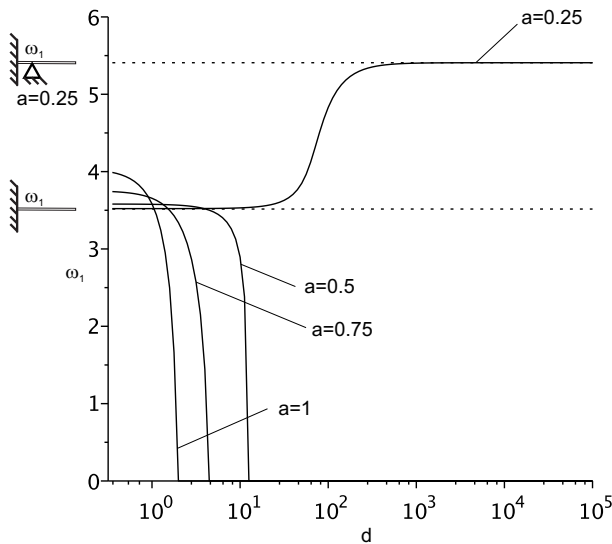


Figure 14. The first natural frequency vs. damping rate for fixed spring rate.

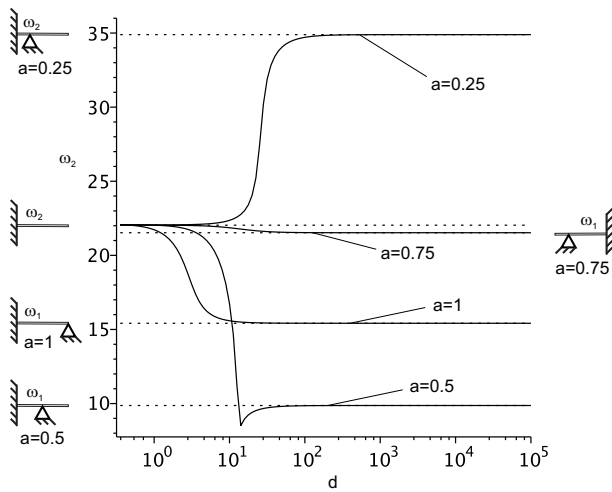


Figure 15. The second natural frequency vs. damping rate for fixed spring rate.

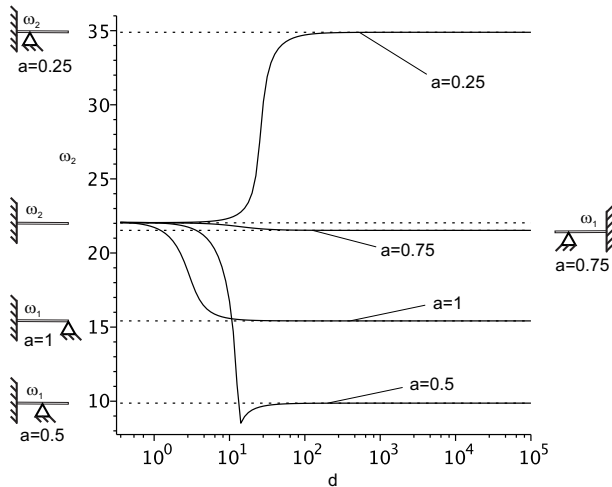


Figure 16. The third natural frequency vs. damping rate for fixed spring rate.

approach is done in [28].

However, we are focussing on long, slender beams, whereby shear forces may have less influence. So, we shall focus on the nonlinear Euler-Bernoulli theory in future work. Additionally, we shall include the conical shape and a precurvature of the beam, neglected until now.

REFERENCES

- [1] M.L. Andermann, J. Ritt, M. Neimark, and C.I. Moore, Neural Correlates of Vibrissa Resonance: Band-Pass and Somatotopic Representation of High-Frequency Stimuli. *Neuron* 42 (2004), pp. 451–463.
- [2] C. Behn, Mathematical Modeling and Control of Biologically Inspired Uncertain Motion Systems with Adaptive Features. Habilitation thesis, Faculty of Mechanical Engineering, Ilmenau University of Ilmenau, Germany (2013).
- [3] A. Birdwell et al., Biomechanical Models for Radial Distance Determination by the Rat Vibrissal System. *The Journal of Neurophysiology* 98 (2007), pp. 2439–2455.
- [4] K. Carl, Technische Biologie des Tasthaar-Sinnessystems als Gestaltungsgrundlage für taktile stiftführende Mechanosensoren, Technical biology of the vibrissa sensor system as design principles for tactile mechanosensors. PhD thesis, Universitätsverlag, Ilmenau (2009).
- [5] J. Dörfel, The musculature of the mystacial vibrissae of the white mouse. *Journal of Anatomy* 135 (1982), pp. 147–154.
- [6] J. Dörfel, The innervation of the mystacial region of the white mouse – A topographical study. *Journal of Anatomy* 142 (1985), pp. 173–184.
- [7] S. Ebara, K. Kumamoto, T. Matsuura, J.E. Mazurkiewicz, and F.L. Rice, Similarities and Differences in the Innervation of Mystacial Vibrissal Follicle-Sinus Complexes in the Rat and Cat: A Confocal Microscopic Study. *The Journal of Comparative Neurology* 449 (2002), pp. 103–119.
- [8] M. Fend, S. Bovet, and H. Yokoi, An Active Artificial Whisker Array for Texture Discrimination. In: *Proceedings of 2003 IEEE/RSJ International Conference on Intelligent Robots and Systems* (2003), pp. 1044–1049.
- [9] M. Fend, Whisker-Based Texture Discrimination on a Mobile Robot. In: *Proceedings of the 8th European Conference on Artificial Life (ECAL)* (2005), pp. 302–311.
- [10] D. Gross, W. Hauger, W. Schnell, and P. Wriggers, Technische Mechanik: Band 4 Hydromechanik, *Elemente der Höheren Mechanik, Numerische Methoden, Technical Mechanics: Volume 4 Hydromechanics, higher mechanics, numerical methods.* Springer, Berlin (2002).
- [11] M. Gürgöze and H. Erol, Determination of the frequency response function of a cantilevered beam simply supported in-span. *Journal of Sound and Vibration* 247(2) (2001), pp. 372–378.
- [12] S. Haidarliu, E. Simony, D. Golomb, and E. Ahissar, Muscle Architecture in the Mystacial Pad of the Rat. *The Anatomical Record* 293 (2010), pp. 1192–1206.
- [13] M.J. Hartmann and J.H. Solomon, Robotic whiskers used to sense features: Whiskers mimicking those of seals or rats might be useful for underwater tracking or tactile exploration. *NATURE* 443 (2006), p. 525.
- [14] S. Hirose, S. Inoue, and K. Yoneda, The whisker sensor and the transmission of multiple sensor signals. *Advanced Robotics* 4(2) (1989), pp 105-117.
- [15] D. Jung and A. Zelinsky, Whisker based mobile robot navigation. In: *Proceedings of the 1996 IEEE/RSJ International Conference on Intelligent Robots and Systems '96 (IROS 96)* (1996), pp. 497–504.
- [16] T.-E. Jin, V. Witzemann, and M. Brecht, Fiber Types of the Intrinsic Whisker Muscle and Whisking Behavior. *The Journal of Neuroscience* 24(13) (2004), pp. 3386–3393.
- [17] D. Kim and R. Möller, Biomimetic whiskers for shape recognition. *Robotics and Autonomous Systems* 55(3) (2007), pp. 229-243.
- [18] M.A. Neimark, M.L. Andermann, J.J. Hopfield, and C.I. Moore, Vibrissa Resonance as a Transduction Mechanism for Tactile Encoding. *The Journal of Neuroscience* 23(16) (2003), pp. 6499–6509.
- [19] S. N’Guyen, P. Pirim, and J.-A. Meyer, Tactile texture discrimination in the robot-rat “Psikharpax”. In: *BIOSIGNALS 2010 – Proceedings of 3rd Int. Conf. on Bio-Inspired Systems and Signal Processing* (2010), pp. 74–81.

- [20] L. Pammer et al., The mechanical variables underlying object localization along the axis of the whisker. *The Journal of Neuroscience: the Official Journal of the Society for Neuroscience* 33(16) (2013), pp. 6726–6741.
- [21] H. Pierson, J. Brevick, and K. Hubbard, The effect of discrete viscous damping on the transverse vibration of beams. *Journal of Sound and Vibration* 332 (2013), pp. 4045–4053.
- [22] T. Prescott, M. Pearson, B. Mitchinson, J. Sullivan, and A. Pipe, Whisking with Robots - From Rat Vibrissae to Biomimetic Technology for Active Touch. *IEEE Robotics and Automation Magazine* 16(3) (2009), pp. 42–50.
- [23] F.L. Rice, A. Mance, and B.L. Munher, A comparative light microscopic analysis of the sensory innervation of the mystacial pad. I. Innervation of vibrissal follicle-sinus complexes. *The Journal of Comparative Neurology* 252 (1986), pp. 154–174.
- [24] R. A. Russell, Closing the sensor-computer-robot control loop. *Robotics Age* 6 (1984), pp. 15–20.
- [25] G. Scholz and C. Rahn, Profile Sensing With an Actuated Whisker. *IEEE Transactions on Robotics and Automation* 20 (2004), pp. 124–127.
- [26] A. E. Schultz, J. H. Solomon, M. A. Peshkin, and M. J. Z. Hartmann, Multifunctional Whisker Arrays for Distance Detection, Terrain Mapping, and Object Feature Extraction. In: *Proceedings of 2005 IEEE International Conference on Robotics & Automation (2005)*, pp. 2588–2593.
- [27] A. K. Seth, J. L. McKinstry, G. M. Edelman, and J. L. Krichmar, Texture discrimination by an autonomous mobile brain-based device with whiskers. In: *Proceedings of the IEEE International Conference on Robotics and Automation (ICRA '04), San Diego, USA (2004)*, pp. 4925–2930.
- [28] J. H. Solomon and M. J. Z. Hartmann, Extracting object contours with the sweep of a robotic whisker using torque information; *The International Journal of Robotics Research* 29 (2010), pp. 1233–1245.
- [29] C. Tuna, J. H. Solomon, D. L. Jones, and M. J. Z. Hartmann, Object shape recognition with artificial whiskers using tomographic reconstruction. *IEEE International Conference on Acoustics, Speech and Signal Processing (ICASSP) (2012)*, pp. 2537-2540.
- [30] N. Ueno, M. M. Svinin, and M. Kaneko, Dynamic contact sensing by flexible beam. *IEEE/ASME Trans. Mechatronics* 3(4) (1998), pp. 254–264.
- [31] D. Voges, K. Carl, G. Klauer, R. Uhlig, C. Behn, C. Schilling, and H. Witte, Structural characterisation of the whisker system of the rat. *IEEE Sensors Journal* 12(2) (2012), pp. 332–339.
- [32] W. Weaver, S. P. Timoshenko, and D. H. Young, *Vibration Problems in Engineering*. John Wiley & Sons Inc., Chichester (1990).
- [33] L. E. Wineski, Facial morphology and vibrissal movement in the golden hamster. *Journal of Morphology* 183 (1985), pp. 199–217.
- [34] H. Yokoi, M. Fend, and R. Pfeifer, Development of a Whisker Sensor System and Simulation of Active Whisking for Agent Navigation. In: *Proceedings of 2004 IEEE/RSJ International Conference on Intelligent Robots and System (2004)*, pp. 607–612.